

Why Are There Tropical Warm Pools?

AMY C. CLEMENT

Rosenstiel School of Marine and Atmospheric Sciences, University of Miami, Miami, Florida

RICHARD SEAGER

Lamont-Doherty Earth Observatory, Columbia University, Palisades, New York

RAGHU MURTUGUDDE

Earth System Science Interdisciplinary Center, University of Maryland, College Park, College Park, Maryland

(Manuscript received 15 November 2004, in final form 17 June 2005)

ABSTRACT

Tropical warm pools appear as the primary mode in the distribution of tropical sea surface temperature (SST). Most previous studies have focused on the role of atmospheric processes in homogenizing temperatures in the warm pool and establishing the observed statistical SST distribution. In this paper, a hierarchy of models is used to illustrate both oceanic and atmospheric mechanisms that contribute to the establishment of tropical warm pools. It is found that individual atmospheric processes have competing effects on the SST distribution: atmospheric heat transport tends to homogenize SST, while the spatial structure of atmospheric humidity and surface wind speeds tends to remove homogeneity. The latter effects dominate, and under atmosphere-only processes there is no warm pool. Ocean dynamics counter this effect by homogenizing SST, and it is argued that ocean dynamics is fundamental to the existence of the warm pool. Under easterly wind stress, the thermocline is deep in the west and shallow in the east. Because of this, poleward Ekman transport of water at the surface, compensated by equatorward geostrophic flow below and linked by equatorial upwelling, creates a cold tongue in the east but homogenizes SST in the west, creating a warm pool. High clouds may also homogenize the SST by reducing the surface solar radiation over the warmest water, but the strength of this feedback is quite uncertain. Implications for the role of these processes in climate change are discussed.

1. Introduction

One of the most prominent features of the tropical oceans is the existence of the warm pools, vast areas of water with relatively homogenous temperatures (Fig. 1a). This feature is well illustrated by the frequency distribution of sea surface temperature (Fig. 1b). There are two important characteristics of this distribution that distinguish the warm pool: First, the distribution is negatively skewed with a peak frequency of SST at 28°C, two degrees below the maximum SST. Second, over 50% of the area in the Tropics has SSTs in the range of $28^{\circ} \pm 1^{\circ}\text{C}$, indicating a high degree of homo-

geneity of SST. These features of statistical distribution of SST are remarkably constant from season to season, and even from year to year (Sobel et al. 2002). In addition to being a defining feature of the tropical oceans, the size and temperature of the warm pool are likely to be important factors in regulating the mean climate and in climate change (Pierrehumbert 1995). At present, there is no theory for what sets these aspects of the warm pool.

The skewness in the distribution of tropical SSTs has previously been interpreted to imply that there is some process that regulates the maximum SST. That is, as the SST approaches a threshold, it is limited from further warming by some regulating mechanism, and as a result there is a clustering of SSTs near that threshold value. Prior studies have suggested different possible regulating mechanisms. Ramanathan and Collins (1991) proposed the existence of a “cirrus cloud thermostat”: as

Corresponding author address: Amy Clement, Rosenstiel School of Marine and Atmospheric Sciences/MPO, University of Miami, 4600 Rickenbacker Causeway, Miami, FL 33149.
E-mail: aclement@rsmas.miami.edu

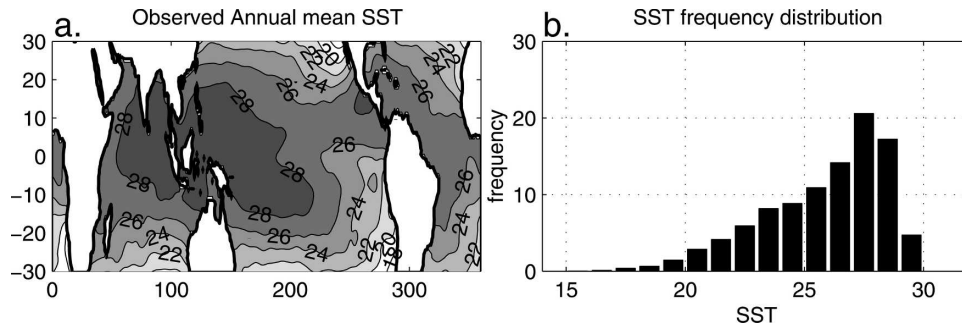


FIG. 1. (a) Annual mean SST ($^{\circ}\text{C}$) from Levitus and Boyer (1994). (b) Frequency distribution for the SST shown in (a) as a percent area (so that the sum of over all SSTs is 100%).

SSTs rise, deep convection ensues and produces highly reflective cirrus clouds that shade the surface and prevent further warming. Waliser and Graham (1993) provided additional observational support for local cooling mechanisms associated with tropical deep convection. These arguments have been disputed in a number of papers that point out that tropical convection is not just a function of local SST and that the large-scale atmospheric circulation is the limiting process (e.g., Fu et al. 1992; Del Genio and Kovari 2002). This argument was elaborated further by Wallace (1992), who pointed out that the skewness in tropical SSTs should arise as a result of highly efficient atmospheric heat transports in the Tropics. He began by considering normally distributed SSTs about some tropical mean that is in radiative–convective equilibrium. The warmest SST would become the preferred site for deep convection, and the effect of enhanced air–sea fluxes in that region would be distributed deep into the troposphere and spread very effectively throughout the Tropics under the constraint that free tropospheric temperature gradients are weak. The cooler SSTs come into a more local equilibrium since these areas are dominated by stable stratification in the atmosphere. Thus, the warmest SSTs are very effectively damped toward the tropical mean value, but the coolest SSTs are not, resulting in a skewed distribution and a homogenous warm pool. These ideas regarding the SST skewness led to other studies that investigated the role of various feedbacks on tropical SST such as surface evaporation (Hartmann and Michelsen 1993; Zhang et al. 1995), free-tropospheric humidity (Pierrehumbert 1995; Larson et al. 1999), and low cloud cover (Miller 1997), and ocean dynamics (Sun and Liu 1996; Clement et al. 1996; Clement and Seager 1999). These studies were generally aimed at elucidating the processes that regulate the tropical mean temperature and not the homogeneity of SST in the warm pool. More recently, Sobel (2003) has revisited the idea that clouds are essential to determin-

ing the spatial structure of the tropical climate. He focused on the somewhat paradoxical collocation of an evaporation minimum and a precipitation maximum over the warm pool and suggested that this could be explained mainly by spatial variations in cloud cover. Though his study does not address how SST is determined, it does imply that clouds are a primary factor in determining the spatial distribution of the surface heat fluxes.

These studies point almost exclusively to atmospheric mechanisms as being responsible for the observed distribution of tropical SST, and thus the existence of a warm pool. The role of the ocean in the establishment of the warm pool has not been addressed explicitly. The effect of ocean dynamics on the east–west asymmetries of the equatorial oceans has been solidly established by decades of theoretical and observational studies (Bjerknes 1966; Wyrtki 1975; Cane and Sarachik 1976; Dijkstra and Neelin 1995; Sun and Liu 1996). Clement and Seager (1999) studied the influence of ocean heat transports on the mean tropical SST but not the distribution. Seager et al. (2003a) looked at the mechanisms in the ocean and atmosphere that give rise to the evaporation minimum on the equator but did not address how these affect the SST. Thus, it is an open question as to what effect the ocean has on producing the homogeneity and broad geographical extent of the warm pool.

The aim of this paper is to provide a more complete framework for understanding the origin of tropical warm pools. Our approach is to identify both the atmospheric and oceanic processes that play a role in creating skewness and homogeneity in tropical SSTs. Without doubt, the oceanic and atmospheric mechanisms of interest arise via coupled interactions, so they cannot be considered truly separately. Here we use an hierarchy of models in order to isolate and quantitatively assess the individual effects of what are, in reality, coupled processes. The way this paper is structured is

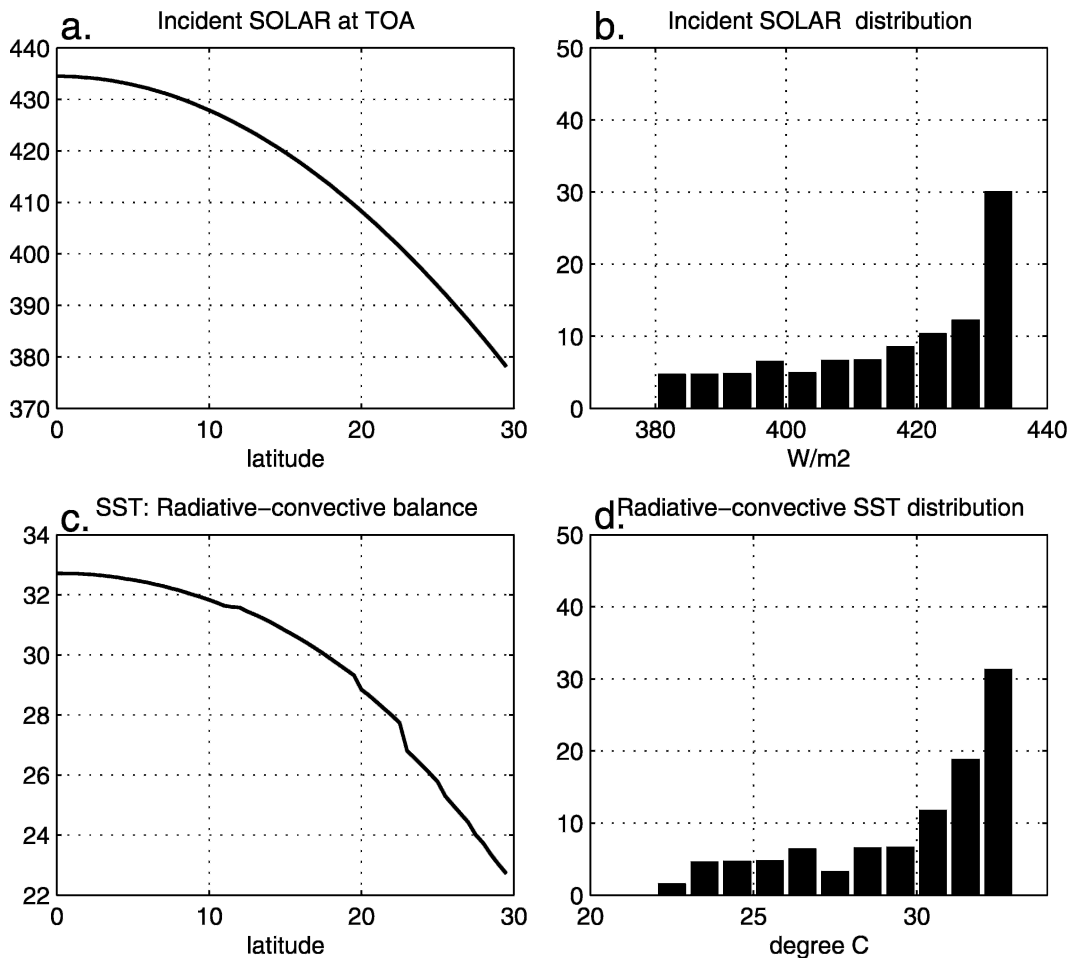


FIG. 2. (a) Annual mean incident solar radiation (W m^{-2}) at the TOA used in the one-dimensional Betts-Ridgway model. (b) Frequency distribution of annual mean incident solar radiation shown in (a). (c) Equilibrium SST ($^{\circ}\text{C}$) computed in the Betts-Ridgway model in response to the incident solar radiation. (d) Frequency distribution for the SST shown in (c).

that we start with the simplest processes and add step by step additional physics in the atmosphere and ocean to see how the SST distribution is altered. Each step requires a particular model. In section 2, we first use a simple one-dimensional model that calculates the local equilibrium SST. In section 3, an atmospheric GCM coupled to a mixed layer ocean model is used to evaluate the impact of nonlocal atmospheric processes on the distribution. In section 4, a simplified ocean model is used to test how oceanic processes contribute. A discussion about the relative importance of atmospheric and oceanic processes, and the possible role of these processes in climate change, is provided in section 5, and conclusions are presented in section 6.

2. The distribution of SST under local balance

As a starting point, we wish to determine the extent to which the features of the observed SST distribution

can be predicted on the basis of the distribution of incoming solar insolation alone. On an annual mean basis, the earth receives maximum solar insolation on the equator and the amount decreases with the cosine of latitude. As such, there is a region within several degrees of the equator over which the annual mean incoming solar radiation [at the top of the atmosphere (TOA)] changes very little (Fig. 2a). If the SST were simply a linear function of the solar radiation, one would expect a skewed distribution in the Tropics with the highest SST being the most common (Fig. 2b).

Local processes such as convection, radiation, surface heat and moisture exchange, etc., however, can alter the relationship between SST and incoming solar radiation. To test how local processes influence the SST distribution, we use the one-dimensional climate model developed for the Tropics by Betts and Ridgway (1989, hereafter BR89). Given the solar radiation, the model

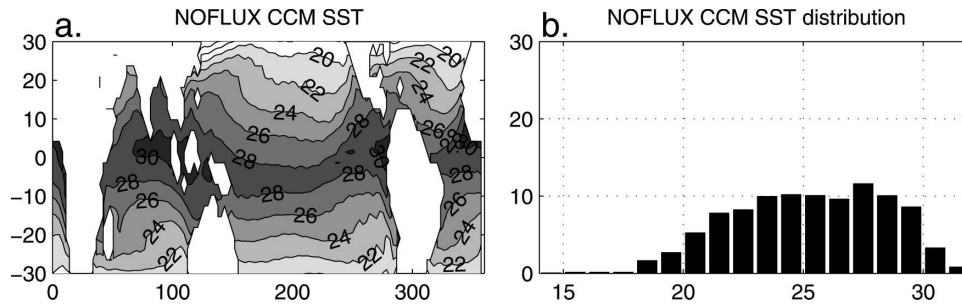


FIG. 3. (a) Annual mean SST from CCM3 experiment in which ocean heat transports are set to zero everywhere. (b) Frequency distribution for the SST shown in (a).

solves for SST and humidity and temperature profiles in the convective boundary layer (CBL) and free troposphere. Because the solar radiation is a unique function of latitude, we run the model for each degree of latitude from 30°S to the equator. Atmosphere and ocean heat transports (which are specified in the BR89 model) are set to zero everywhere to ensure that the resultant SST is due to purely local processes. A CBL cloud fraction of 25% and a wind speed of 6.7 m s^{-1} are specified at all latitudes. (These were the tropical mean values used in BR89. The results of relevance to this study are not affected by the choice of these values.) The SST as a function of latitude for the BR89 model is shown in Fig. 2c. The BR89 SST has approximately the same latitudinal structure as the incoming solar radiation, as well as a similar skewness (Fig. 2d), implying that local radiative–convective processes do no more to homogenize tropical SST (with latitude) than is already done by the solar radiation.

These results reveal that, on the basis of the incoming solar radiation alone and only local feedbacks in the atmosphere, one would expect a highly skewed tropical SST. This case is, however, unlike the observed distribution in which the peak frequency of SST is not the highest but is two degrees below the maximum SST (Fig. 1b). The rest of this paper will examine how non-local atmospheric and oceanic processes alter the local equilibrium SST distribution to produce the observed one. We contend that this is a more useful starting point than taking the normally distributed SST of Wallace (1992). It is not the damping of the highest SSTs of a normal distribution that needs an explanation, but rather the shift from an extremely skewed distribution of local equilibrium (Fig. 2d) to a slightly more normal distribution with a peak frequency below the maximum SST (Fig. 1b).

As a final point we note that, if random noise were added to the distribution of solar radiation or SST shown in Fig. 2, the skewness would be reduced and the peak would shift to lower values, more closely resem-

bling the observed distribution. However, it is clear that the deviation of the observed annual mean SST from that which would be expected on the basis of solar radiation alone is not random. Rather, it has a distinct spatial structure that is clearly tied to physical mechanisms, and it is the goal of the rest of this paper to identify those mechanisms.

3. Can the atmosphere create a warm pool on its own?

All explanations proposed to date for the existence of tropical warm pools have involved atmospheric mechanisms. Here we test the ability of the atmosphere to create warm pools by performing an experiment with an atmospheric general circulation model (AGCM). The atmosphere model is the Community Climate Model (CCM3) atmospheric GCM described in Kiehl et al. (1998). The model is run with a spectral truncation of T42, which corresponds to an approximate horizontal resolution of 2.8° latitude by 2.8° longitude, and there are 18 vertical levels. The model is coupled to a mixed layer ocean in which the SST is computed. It is common in such a model configuration to implicitly include the effects of ocean heat transports by adding a term to the SST equation that is designed to force the SST to be close to the observed. Here, we wish to isolate the effects of atmospheric processes, so we do not include such a correction. As such, in equilibrium the annual mean SST is that which ensures zero net surface heat flux. This experiment allows the atmospheric circulation to interact with local processes to balance the incoming solar radiation. As a result of these processes, the distribution of tropical SST (Fig. 3) is radically altered from the local balance and now shows neither skewness nor a primary mode of SST (i.e., the distribution is flat). Thus, despite the introduction of skewness and homogeneity by the solar forcing, when the atmospheric circulation is allowed to interact (in the absence of ocean heat transport), the skewness is removed and

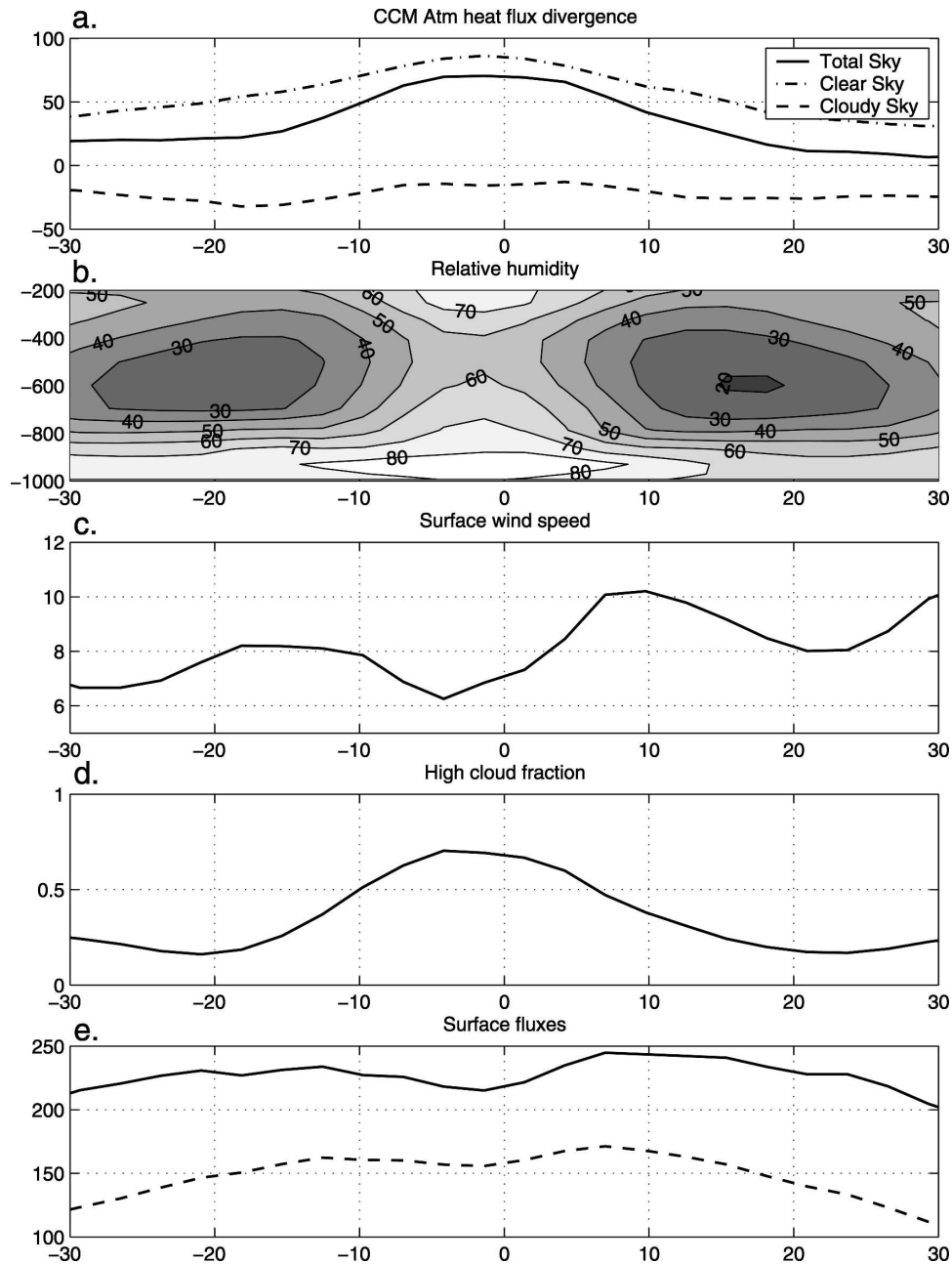


FIG. 4. Zonal average annual mean atmospheric heat flux divergence for each latitude (net heating at the TOA minus the surface; in W m^{-2}) for the CCM3 experiment with no ocean heat transport. The solid line shows the total, the dot-dashed line shows the clear-sky values, and the dashed line shows the cloudy-sky values (positive indicates net heating). (b) Zonal average atmospheric relative humidity (in %). (c) Wind speeds (m s^{-1}) zonally averaged over all ocean points. (d) High cloud fraction. (e) Surface fluxes (W m^{-2}) zonally averaged over all ocean points. The solid line shows the net solar flux (positive downward), and the dashed line shows the latent heat flux (positive upward).

there is, in effect, no region of homogenous SSTs or warm pool.

The change in SST distribution from the local adjustment case (Fig. 2) is ultimately related to the atmospheric circulation. The meridional gradient in incom-

ing solar radiation at the top of the atmosphere drives a circulation that transports heat poleward. This heat transport is accomplished almost entirely by the zonal mean circulation, the Hadley cell (Pierrehomme and Oort 1992). The circulation not only transports heat, but also

alters the cloud, water vapor, and surface wind distribution (Fig. 4), all of which impact the SST. Here we explain the effects on the SST distribution of each of these individual processes in terms of its ability to homogenize, or remove homogeneity, from the tropical SST.

First, let us consider the influence of atmospheric heat transports on SST. As shown in Fig. 4, the atmospheric heat flux divergence is a maximum on the equator. The atmosphere removes heat preferentially from the warmest regions and, hence, would, on its own, tend to homogenize the SST. To illustrate this, we return to the BR89 model. The atmospheric heat transport is a specified parameter in that model, which was set to zero in the previous section to examine the local balance. Here, we allow the heat transport to vary with the atmospheric temperature, and it is parameterized as $xa = 5 \text{ W m}^{-2} \text{ K}^{-1} (\langle T \rangle - 250 \text{ K})$, where $\langle T \rangle$ is the column-mean temperature and 250 K is taken as a typical mid-latitude column-mean temperature. We use a scale factor of $5 \text{ W m}^{-2} \text{ K}^{-1}$, the value of sensitivity of atmospheric heat transport to warm pool temperature calculated by Clement and Seager (1999) using a box model framework for the tropical climate. The resulting SST distribution is compared with the local balance case from the previous section in Figs. 5c,d. The computed atmospheric heat transport is maximum on the equator and decreases to zero at 30° latitude, which tends to homogenize the SST by preferentially cooling the warmest SST. The resulting SST distribution (Fig. 5d) has a similar shape as observed with a peak at values below the maximum SST, but the range is significantly reduced. Hence, it appears that the effect of atmospheric heat transport does, indeed, tend to homogenize the SST, as suggested by Wallace (1992). However, as shown in Fig. 3, the GCM does not have a distribution like this, so other atmospheric processes must overwhelm this effect.

Atmospheric relative humidity in the GCM is shown in Fig. 4b. The effect of the Hadley circulation causes drying of the subtropical free troposphere. This dynamical drying of the subtropics has been discussed in previous studies (Salathe and Hartmann 1997, 2000; Herweijer et al. 2005) and also appears to operate on interannual time scales in response to ENSO-driven changes in Hadley cell strength (Soden 1997). The drying in the subtropics lowers the atmospheric greenhouse trapping in that region, which results in a cooler SST (Herweijer et al. 2005). To illustrate how this affects the SST distribution quantitatively, we modified a parameter, T_{crit} in the BR89 model, that alters the relative humidity above the trade wind inversion. Briefly, this parameter is used to set the above inversion spe-

cific humidity as $q_T = q_s(T_{\text{crit}}, \theta_E)$, where θ_E is the subcloud layer equivalent potential temperature. In the previous section on local balance, T_{crit} was set to a constant value of 266 K. Now we specify a latitudinally varying T_{crit} in order to account for the effect of dynamical drying on SST. Figures 5e,f show the SST distribution for T_{crit} decreasing linearly from 276 K on the equator to 255 K at 30° latitude. This corresponds to a decrease in inversion relative humidity from 60% to 40%, comparable to the relative humidity changes at 800 mb in the GCM (Fig. 4b). Because of the reduced greenhouse effect in the subtropics, the SST is considerably lower, and hence is distributed over a wider range. However, the SST distribution is still peaked and does not have the range of that in the GCM (Fig. 3). The atmospheric heat transport in this case (Fig. 5e) is 40 W m^{-2} on the equator and zero at 30° , comparable to the meridional decrease of 60 to 20 W m^{-2} in the GCM (Fig. 4a). (We do not account for the 20 W m^{-2} cooling of the entire Tropics in the GCM because this affects the mean, but not the distribution.) The equatorial heat transport is larger in this case than in the case with constant T_{crit} (Fig. 5c), which reflects the fact that the amount of heat transport is tied to the distribution of humidity in the atmosphere.

The final factor to consider in order to understand the GCM SST distribution is the surface wind speed. Unlike the local equilibrium case shown in section 2 (Fig. 2) where the surface wind speeds were set to be constant, when the atmosphere is allowed to circulate in response to the distribution of solar radiation, the surface wind speeds become significantly nonuniform (Fig. 4c). This distribution of wind speed has a similar structure to the observed (Fig. 7) with maxima off the equator in the core of the trade winds, though the overall wind speed is higher due to the stronger Hadley circulation. To evaluate the effect on the SST distribution, the wind speeds are varied in BR89 from 5 m s^{-1} on the equator to 9 m s^{-1} at 30° . This case has interactive latitudinally varying atmospheric heat transport, varying T_{crit} , as well as varying wind speeds, and the resulting SST is shown in Figs. 5g,h. With the inclusion of all these effects the distribution is flat with a range comparable to that in the GCM (Fig. 3). The effect of wind speed on SST has been discussed in Seager et al. (2000). Those authors showed that, as wind speed increases, the thermodynamic state of the atmosphere moves closer toward that of the ocean as the air – sea temperature difference is decreased. The warmer and moister atmosphere radiates more to space and, to restore equilibrium, the SST cools. Low wind speeds on the equator therefore lead to warmer SSTs and high wind speeds off the equator lead to cooler SST, thereby

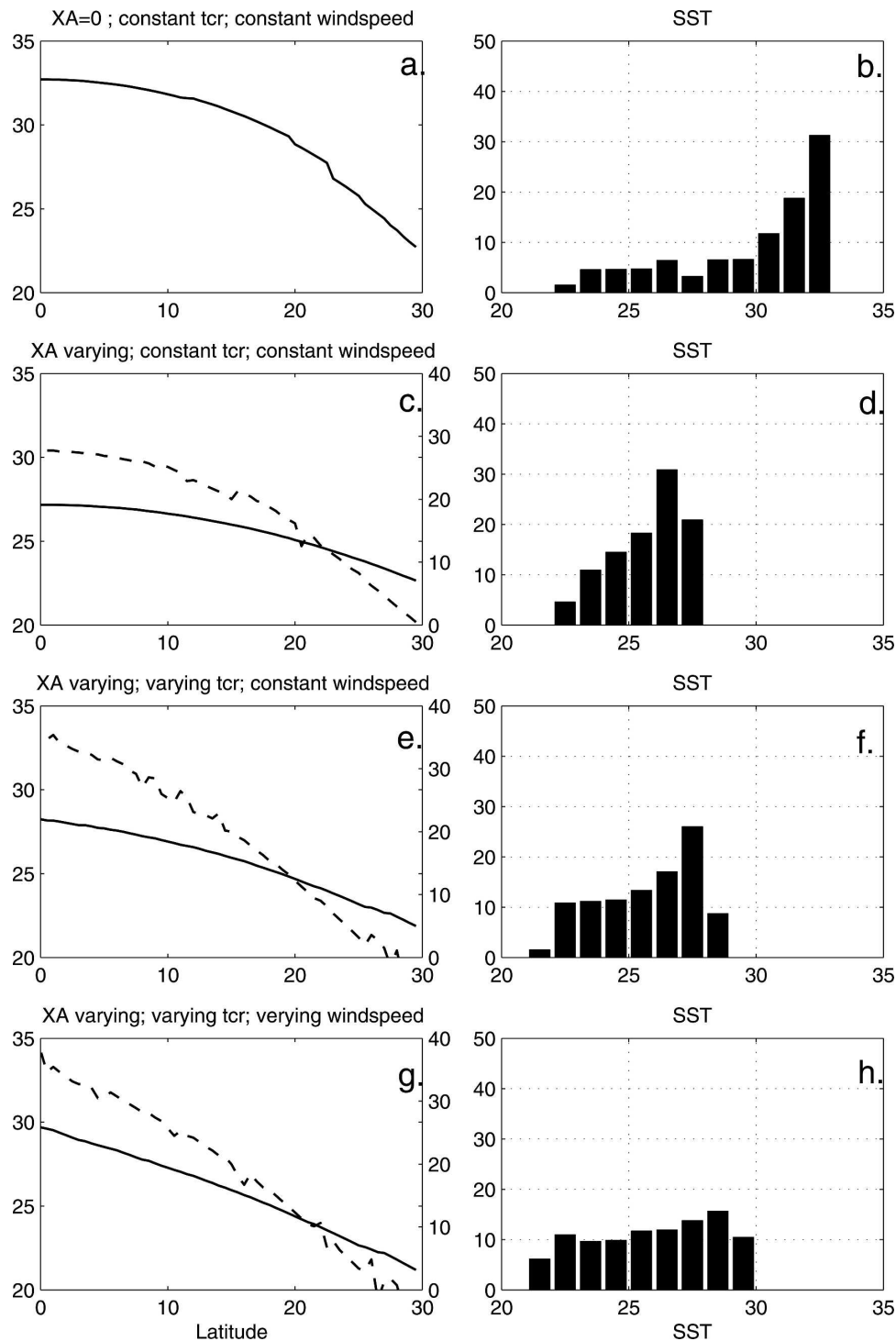


FIG. 5. Results from the Betts–Ridgway model showing the relative effects of atmospheric heat transport, atmospheric humidity, and surface wind speeds on the SST distribution. (a) SST as a function of latitude for the case for local balance with atmospheric heat transport set to zero and T_{crit} and surface wind speed constant. (b) Frequency distribution for the SST shown in (a). (c) SST (solid, left axis) and atmospheric heat export in W m^{-2} (dashed, right axis) for the case of interactive atmospheric heat transport and T_{crit} and surface wind speed constant. (d) Frequency distribution for the SST shown in (c). (e) SST (solid, left axis) and atmospheric heat export in W m^{-2} (dashed, right axis) for the case of interactive atmospheric heat transport, T_{crit} varying with latitude, and surface wind speed constant. (f) Frequency distribution for the SST shown in (e). (g) SST (solid, left axis) and atmospheric heat export in W m^{-2} (dashed, right axis) for the case of interactive atmospheric heat transport and T_{crit} and surface wind speed varying with latitude. (h) Frequency distribution for the SST shown in (g).

removing homogeneity and resulting in a flat SST distribution, as in the GCM (Fig. 3). The addition of variations in wind speed does not alter the atmospheric heat transport by much because, while SST changes are significant, atmospheric temperature changes are smaller in response to altered wind speed (Seager et al. 2000).

To summarize, we find that the atmosphere adjusts to the distribution of solar radiation via processes that both tend to homogenize and remove homogeneity from the tropical SST distribution, and the sum of these effects is a flat SST distribution, with no preferred SST (or warm pool) at all, as shown in Figs. 3 and 5g,h. The circulation on its own tends to smooth out SST gradients via the heat transport, which preferentially cools the warmest SSTs on the equator where solar radiation is greatest. However, the circulation also results in a moist deep convective region with low wind speeds and dry subtropics with high wind speeds. These latter effects increase meridional SST gradients by changing the greenhouse trapping and the air – sea temperature difference in different regions of the atmosphere. The humidity and wind speed distributions appear to be the dominant effects in setting the meridional SST distribution in the GCM. We note that using the BR89 model to test these relative effects has the shortcoming that they are not fully interactive (as they are in the model and, of course, the real atmosphere). Moreover, it is not known what the true sensitivities of SST are to these various processes. However, these simple experiments are useful in that they illustrate how the relative influence of the *quantitative* changes in heat transport, humidity, and winds in the GCM affect the SST distribution.

One additional effect that we have not yet discussed is the role of clouds. It is difficult to determine quantitatively what effect clouds have on the SST distribution. There is little meridional structure in the net cloud forcing at the TOA (Fig. 4a), which would seem to suggest that the clouds do little to alter the distribution. This is not because there is no meridional structure in the clouds—high clouds have a very distinct peak on the equator (Fig. 4d)—but rather because high clouds have compensating effects on the TOA shortwave and longwave fluxes. Although the net TOA effect of these clouds is small, they do have a significant effect on the surface energy budget. There is a minimum in surface solar radiation on the equator that is balanced by a minimum in latent heat flux (Fig. 4e). By reducing the solar radiation over the warmest waters, clouds tend to homogenize the distribution of SST, as envisioned by Ramanathan and Collins (1991), whereby the warmest SSTs are cooled by cloud shading. However, a number of caveats apply here: First, Hartmann et al. (2001)

have shown that it is actually an ensemble of clouds types that give rise to the TOA cancellation, making the connection between SST and high clouds even more complicated. Moreover, there is no clear local relationship between SST and clouds (Hartmann and Michelsen 1993; Lau et al. 1994; Larson and Hartmann 2003; Del Genio and Kovari 2002). Thus, while we can argue qualitatively that high clouds will tend to cool the warmest SST, the quantitative relationship remains rather unclear.

The absence of homogeneity and skewness in this experiment is not particular to the CCM. In identical experiments performed by Clement and Seager (1999) with the Goddard Institute for Space Studies (GISS) Model II', and with the latest version of the Geophysical Fluid Dynamics Laboratory (GFDL) atmosphere model (Winton 2003), the distribution of tropical SST in the case with no ocean heat transport was flat, as in Fig. 3. In all models, the adjustment of the atmosphere to the distribution of solar radiation is basically the same with a strong Hadley circulation, dry subtropics, high off-equatorial wind speeds, and strong tropical SST gradients. This result is sufficiently robust that it does not depend on the details of the model physics, which are quite different in these models.

4. Oceanic mechanisms in the establishment of warm pools

Now that we have considered both local and nonlocal processes in the atmosphere, we wish to investigate how the ocean contributes to the adjustment of the tropical SST under the incoming solar radiation. The atmospheric circulation that arises in response to the distribution in solar radiation results in a surface wind stress that drives the circulation of the ocean. How does the ocean response to the surface winds influence the distribution of tropical SST?

To answer this question, we construct a simplified model of the tropical ocean. The model is a 1.5 layer model, and the thermocline depth is computed according to Sverdrup dynamics as in Veronis (1973). The SST is computed within an embedded fixed-depth 50-m mixed layer accounting for horizontal ocean advection, upwelling, and surface heat fluxes. These are all formulated as in Seager et al. (1988), as is the total surface current, which includes Ekman plus Sverdrup contributions. A parallel integration is performed in which the SST is computed for purely local balance. The difference between this local SST and that for the dynamical model provides the total contribution of ocean dynamics to the SST. Solar forcing, wind speed, and wind stress are specified at annual and zonal mean values. See the appendix for complete model details. The

model is configured to reproduce the Pacific Ocean, which makes up the majority of the area of the tropical oceans. Application of the findings to the Atlantic and Indian Oceans is also discussed.

The effect on the SST skewness of the different processes shown thus far can be clearly illustrated within the framework of the simple model. First, let us consider the case of local balance in the Pacific: constant clouds and constant surface wind speeds (6.7 m s^{-1}) are specified and only the solar radiation varies with latitude. The resultant SST map and distribution (Figs. 6a,b) are qualitatively consistent with the results of the BR89 calculations (Fig. 2) where there is significant skewness and the most common SST is at the highest value (over 30°C). Next, we retain local ocean balance but use the observed wind speed distribution from the da Silva et al. (1994) dataset in the calculation of the surface fluxes. To keep matters simple, we use the zonal mean values shown in Fig. 7. As shown in Figs. 6c,d as a result of the low observed wind speeds on the equator and higher wind speeds off the equator, the meridional SST gradient is increased and the skewness is removed. The effect of the midtropospheric humidity distribution, which was shown to be important in lowering the off-equatorial SSTs in the atmospheric GCM, is not included explicitly in this model because of the simplicity of the surface heat flux formulation (see the appendix). However, the high wind speeds are sufficient to mimic the increased heat loss from the surface in the off-equatorial region, and the result is a distribution comparable to that of the GCM (Fig. 3).

Next, we allow ocean dynamics to respond to the zonal wind stress. Figure 6e shows the contribution of ocean dynamics to the total SST in the case where the observed zonal mean wind speed and zonal mean wind stress are imposed. Ocean dynamics cool the equatorial regions where the SST is high and warm the off-equatorial region where the SST is lower. This dynamical contribution is the combination of two different ocean processes. Easterly wind stress drives equatorial upwelling and poleward Ekman drift across the entire basin, which transports heat poleward. Also under easterly winds, the equatorial thermocline develops an east–west tilt (Cane and Sarachik 1976). As such, in the west, the upwelled subsurface water that replaces the water advected poleward by Ekman drift is relatively warm. There, ocean dynamics reduce the SST of the very warmest water and increase the SST of the cooler water, producing a region of homogenous SSTs—the warm pool. The same meridional overturning in the east, where the equatorial thermocline is shallow, brings cold water to the surface, creating a cold tongue. The net surface heat flux in the simple ocean model

(Fig. 8) is consistent in both spatial pattern and magnitude with ocean heat transports by various estimates, which shows that heat is diverged in the equatorial region and converged in the subtropics (Trenberth and Caron 2001; Seager et al. 2003a). In spite of the simplicity of the ocean physics and the atmospheric forcing, this model reproduces the main features of the warm pool: a broad meridional extent of the water that has a temperature below the maximum value (Figs. 6f,g).

a. Relative roles of Ekman and Sverdrup dynamics

The model contains both Ekman and Sverdrup dynamics. Here we wish to determine how these individual processes contribute to the statistical distribution of SST. The effect of the Sverdrup contribution can be varied by changing the depth of the thermocline on the eastern boundary, h_e , an external parameter that is specified (Veronis 1973). This results in a change in the mean depth of the equatorial thermocline, though the tilt is still determined by Sverdrup dynamics. Large values of h_e result in a deeper thermocline everywhere, but under easterly wind stress it is deeper in the west than the east. The results shown in Fig. 6 used a value of 50 m, close to the observed value.

Figure 9 shows the results for values of $h_e = 50, 100,$ and 200 m . As the mean thermocline deepens, the warm pool expands eastward, as expected, because the temperature of the water upwelled in the eastern basin increases. With $h_e = 200 \text{ m}$, there is no cold tongue, and the distribution of SST becomes extremely skewed with the most common SST at the highest value. It should be noted that, while this is similar to the local balance case with constant wind (Fig. 2), it is for a different reason. For the local case with varying wind speed, the distribution of SST is almost completely uniform as shown in Figs. 6c,d. With ocean dynamics and a deep thermocline the Sverdrup component has little influence on the SST, but Ekman dynamics moves water poleward that otherwise would be extremely warm. This homogenizes the SST at all longitudes, introducing a peak back into the distribution relative to the local balance, though the peak is at the highest value. For smaller values of h_e , the thermocline is shallower and equatorial upwelling cools the SST on the equator in the eastern basin, making the distribution more normal (relative to the deep thermocline case) and closer to the observed distribution. Hence, both Ekman and Sverdrup processes appear to be important in setting the observed distribution: Ekman dynamics homogenize SST by cooling the warmest SST on the equator and warming the off-equatorial regions. This results in a peaked, but highly skewed SST distribution. Sverdrup dynamics

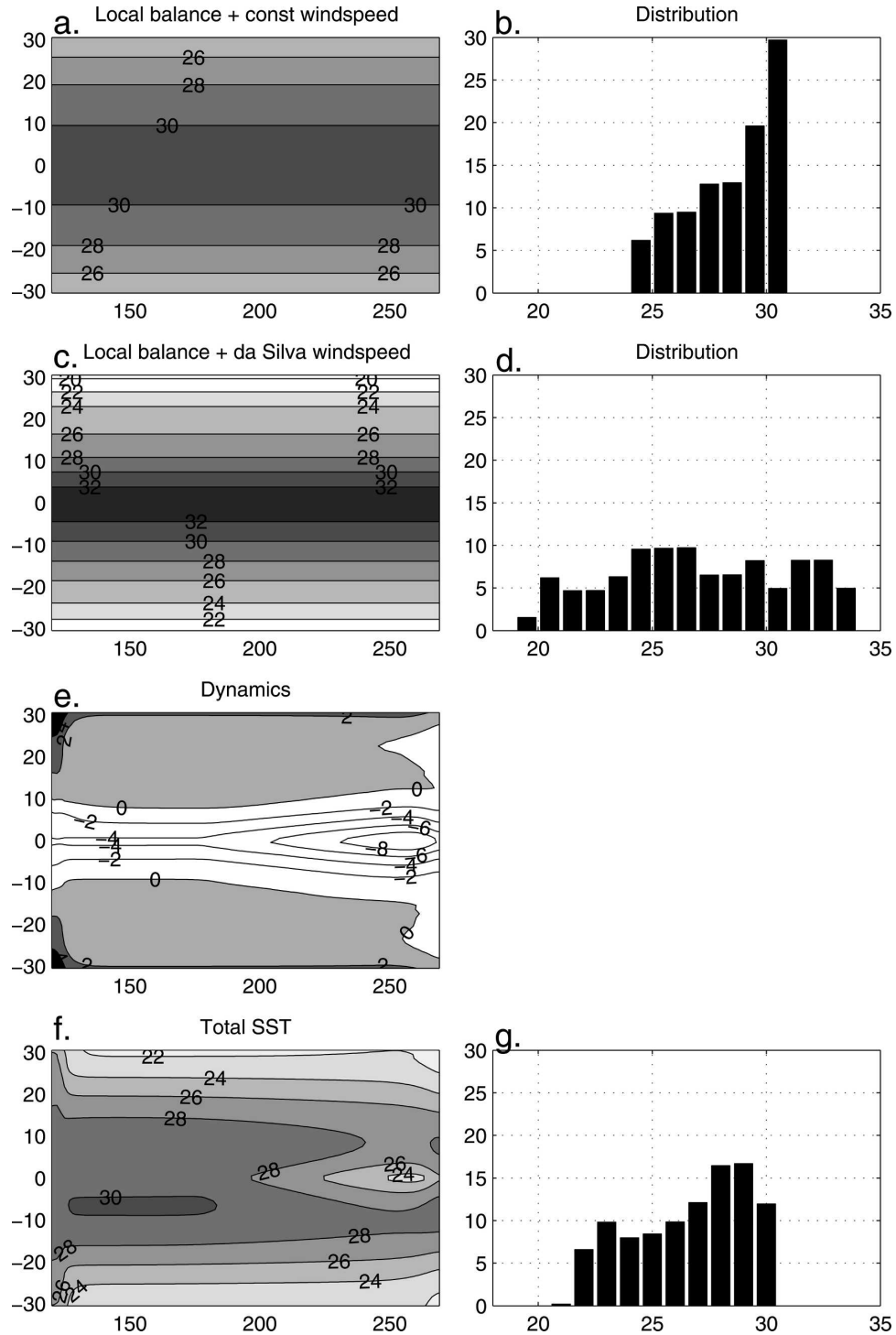


FIG. 6. Results from the simplified ocean model for the Pacific Ocean. (a) Map of the local SST (the effect of dynamics not included) for the case with constant wind speed and constant cloud everywhere. Solar radiation is a function only of latitude. (b) Frequency distribution for the SST shown in (a). (c) Local SST for the case in which clouds are constant, but wind speeds (from the da Silva et al. 1994 dataset) vary as a function of latitude. (d) Frequency distribution for the SST shown in (c). (e) Contribution of ocean dynamics to the SST for the case in which clouds are constant, but wind speeds vary as a function of latitude. (f) Total SST [local shown in (c) plus ocean dynamics contribution shown in (e)] for the case in which wind speeds vary as a function of latitude. (g) Frequency distribution for the SST shown in (f).

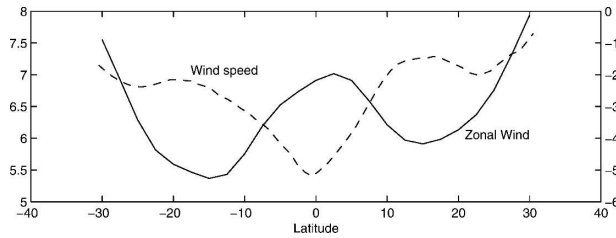


FIG. 7. Zonal wind (solid-axis labeled on right) and surface wind speed (dashed-axis labeled on left) averaged over the Pacific Ocean from the da Silva et al. (1994) dataset as a function of latitude. Both are in m s^{-1} .

shift the peak in the SST distribution toward cooler values by bringing cold water close to the surface in the eastern equatorial Pacific where it can be entrained into the mixed layer. Clearly the Sverdrup circulation is also key to determining the geographical structure of the warm pool, which may explain why the warm pools in each basin are quite different in structure (Fig. 1). In the Indian Ocean, the thermocline is deep all along the equator, and hence the region of homogenized SST extends to nearly all longitudes. In the Atlantic, the thermocline is shallower, and the warm pool is confined to the very western and off-equatorial parts of the basin.

b. The role of clouds

While it appears that Ekman and Sverdrup dynamics are capable of explaining the main features of the SST distribution, there is likely some additional effect on the distribution from clouds. Ramanathan and Collins (1991) pointed out that high clouds overlie the warmest SSTs and reduce the incident surface solar radiation there. This feedback appears to operate in the GCM (Fig. 4e), but the effect of clouds on the SST distribution has not been quantified. While studies subsequent to Ramanathan and Collins (1991) showed that the feedback between high clouds and SST is not a simple one and depends on spatial gradients of SST rather than local SST (Fu et al. 1992; Lau et al. 1994; Hartmann and Michelsen 1993; Del Genio and Kovari 2002), there is an observed positive correlation between SST and deep convective cloud cover and cloud properties for the annual mean climatology (Hartmann et al. 1992; Del Genio and Kovari 2002). Here we can use the framework of the simple ocean model to illustrate the effect of high clouds on the SST distribution. A cloud feedback is parameterized in the simplest possible way: For values of SST within two degrees of the maximum SST over the entire domain, the surface solar radiation is reduced. The amount by which it is reduced scales as a specified value dQ_s/dT per degree Celsius above the value of the maximum SST minus 2°C . We note that this differs from the cirrus cloud feedback envisioned

by Ramanathan and Collins (1991) where a threshold for convection was reached at 27.5°C . This removes the dependence of the cloud feedback on an absolute value of temperature, hence allowing the feedback to have the same effectiveness irrespective of the tropical mean SST. Figure 10 shows the SST distribution for values of $dQ_s/dT = 0, 8, 15,$ and $25 \text{ W m}^{-2} \text{ K}^{-1}$. To isolate the effect of the clouds, ocean dynamics are not included (for now). The wind speeds do vary with latitude in order to illustrate the relative roles of the atmospheric circulation and clouds on the distribution. For a value of $dQ_s/dT = 0$, there is no cloud feedback and the local SST distribution is the same as shown in Fig. 6d with no peak. As the value of dQ_s/dT increases and the feedback becomes stronger, the distribution becomes more like the observed with a peak developing below the maximum SST. This demonstrates that cloud feedbacks are capable of homogenizing SST and reproducing the skewness in the observed distribution. The question is: What is the strength of this feedback; that is, what is a realistic value for dQ_s/dT ?

Ramanathan and Collins (1991) used interannual variations in surface temperature to calculate a tropical average of the quantity, $dC_s dT/dT^2$ (where C_s is the top-of-atmosphere cloud shortwave forcing and T the surface temperature) and found it to be in the range from 22 to $27 \text{ W m}^{-2} \text{ K}^{-1}$. More recent studies have suggested that this value probably overestimates the strength of the cloud feedback because it does not isolate the local connection between SST, vertical motions, and clouds relative to nonlocal contributions (Fu et al. 1992; Lau et al. 1994; Del Genio and Kovari 2002). A simple correlation of the climatological SST and cloud shortwave forcing measured during the Earth Radiation Budget Experiment (ERBE) yields a value of $15 \text{ W m}^{-2} \text{ K}^{-1}$ for values of SST over 27°C , though, again, this may be considered an upper limit since it does not account for the correlation between SST and vertical velocities or different cloud types. In the CCM experiment, shown in Figs. 3 and 4, the strength of the cloud feedback calculated in the same way is $8 \text{ W m}^{-2} \text{ K}^{-1}$, about half the observed value. The SST distribution from the simple model using this parameter value (dotted-dashed line in Fig. 8) is consistent with that from the atmospheric GCM (Fig. 3b) where there is a shoulder in the distribution at the highest SSTs but no strong peak. In this case, high off-equatorial wind speeds produce large meridional gradients, and the cloud feedback is not strong enough in the model to lower the warmest SST and smooth out those gradients. If the feedback in CCM was the full strength of the observed (i.e., $15 \text{ W m}^{-2} \text{ K}^{-1}$), the results shown here suggest that, while that cloud feedback would introduce

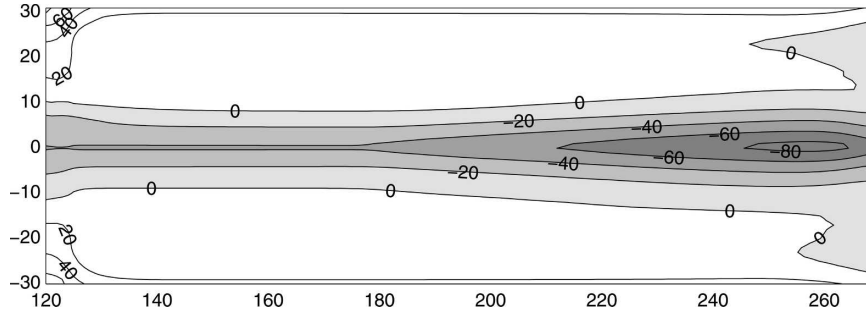


FIG. 8. Net surface heat flux (W m^{-2}) in a simple model (defined as positive upward). Contour interval is 20 W m^{-2} .

a peak in the distribution, it would not be as peaked as the observed distribution.

The way in which we have parameterized the cloud feedback in this model is admittedly oversimplified. It is not presently known what the quantitative relationship is between SST and shortwave forcing of high clouds. Moreover, Hartmann et al. (2001) have shown that the net top-of-atmosphere cloud forcing in con-

vecting regions is related to not just one cloud type, but to an ensemble of cloud types, which is obviously not possible to include in such a simple model framework. However, the results shown in Fig. 10 are useful for illustrating how a simple cloud feedback can counter the effect of surface wind speeds on the SST distribution to produce a distribution with some of the observed features.

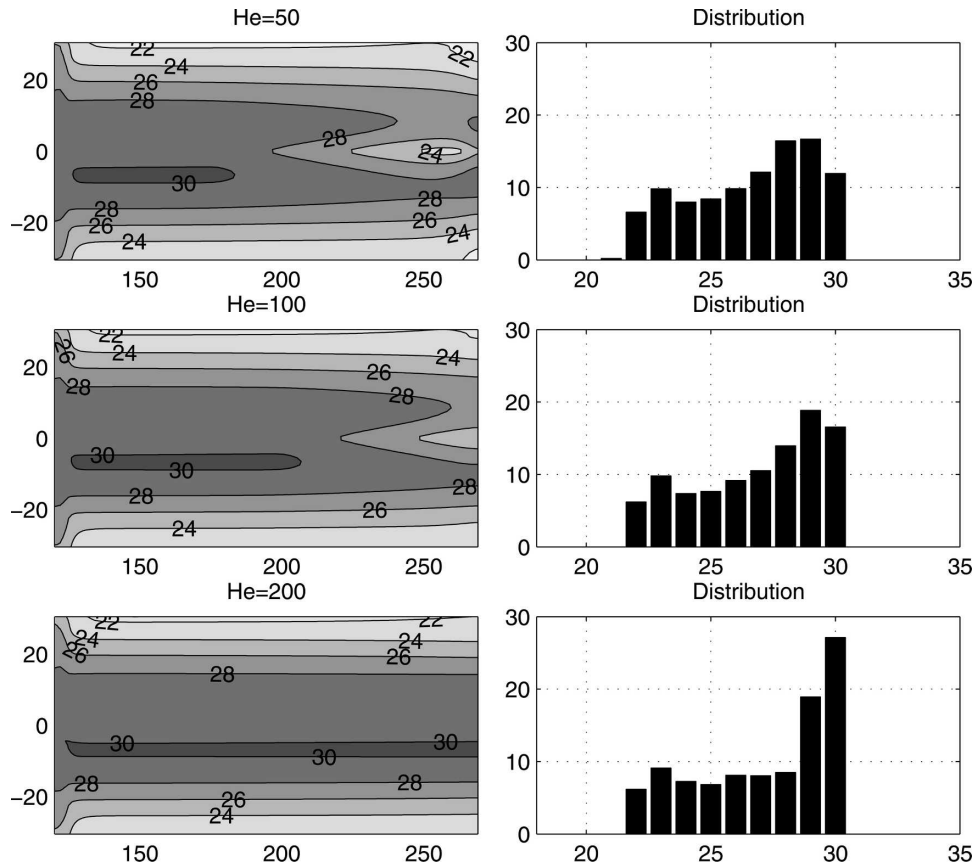


FIG. 9. Results from the ocean model in which h_e , the depth of the thermocline at the eastern boundary, is varied. (top) The map and distribution for $h_e = 50 \text{ m}$, which is close to the observed value, and was the value used for results shown in Fig. 5; (middle) for $h_e = 100 \text{ m}$; and (bottom) for $h_e = 200 \text{ m}$.

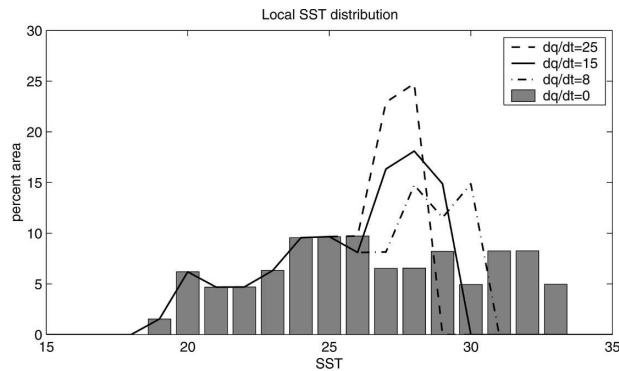


FIG. 10. Results from the ocean model in which the simple cloud feedback is included. The effects of ocean dynamics are not included, so what is shown are the local SSTs. The bars show the distribution for the case in which wind speeds vary with latitude, but cloud feedback is not included ($dQ_s/dT = 0$). The dotted-dashed curve shows the case for $dQ_s/dT = 8 \text{ W m}^{-2} \text{ K}^{-1}$, which is about the value in the CCM experiment without ocean heat transports; the solid line shows the case for $dQ_s/dT = 15 \text{ W m}^{-2} \text{ K}^{-1}$, similar to the value derived from observations; and the dashed line shows the case for $dQ_s/dT = 30 \text{ W m}^{-2} \text{ K}^{-1}$, a more extreme value at the upper end of the range suggested in the literature.

c. Summary

To summarize, the results show that both ocean dynamics and cloud feedbacks can explain the main features of the observed SST distribution. However, with parameters that are justified by the observations ($h_e = 50 \text{ m}$ and $dQ_s/dT = 15 \text{ W m}^{-2} \text{ K}^{-1}$), neither process can

individually explain the full magnitude of the peak in the SST distribution (Fig. 6g for ocean dynamics and Fig. 10 for high clouds). One final experiment with the simplified model illustrates that the combination of these two processes yields a SST distribution that is in agreement with the observed (Fig. 11). We note, however, that these processes are not capable of explaining the cold tail of the distribution of observed SST, which arises because of the low SSTs that occur in the eastern subtropics and extend onto the equator in the southeastern Pacific. Seager et al. (2003b) showed that the eastern subtropical SST is determined by a mixture of atmosphere and ocean processes, both dynamical and thermodynamic. Moreover, those authors showed the importance of the seasonal cycle in the eastern ocean basins, while we have only analyzed processes operating in an annual mean sense. Another important climatic factor that is missing from this study is the role of low-level stratus clouds in the eastern Pacific. It is well known that these clouds both contribute to and are influenced by the cold SSTs that they overlie (Klein and Hartmann 1993; Ma et al. 1996; Seager et al. 2003b). However, most GCMs do not simulate stratus clouds satisfactorily, and the role of these clouds in climate feedbacks is the subject of active, ongoing research. Thus, while the warm end of the tropical SST distribution can be explained with a relatively simple set of physical mechanisms evaluated on an annual mean basis, simulation of the full distribution of tropical SST, in

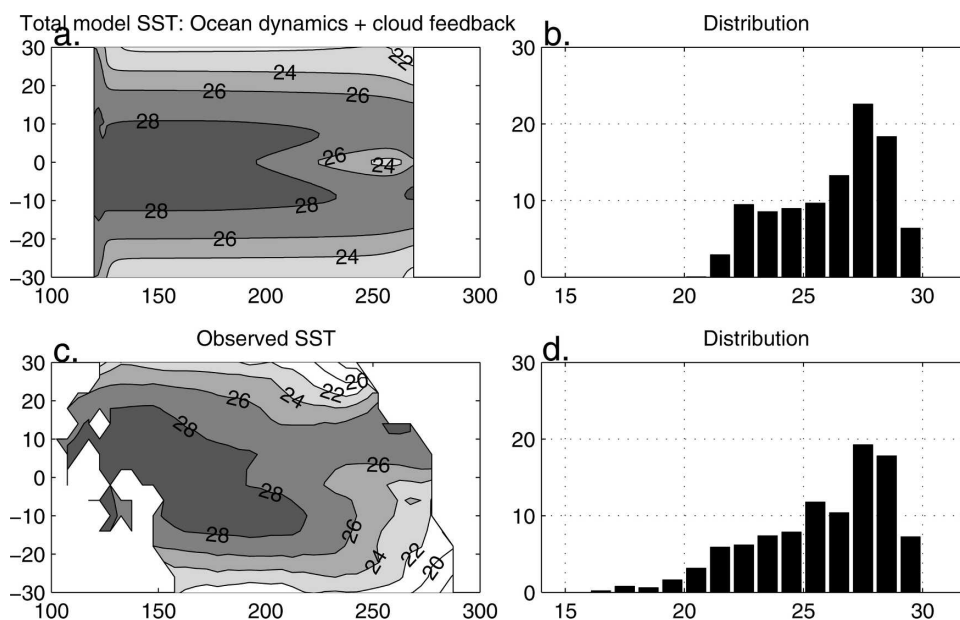


FIG. 11. (top) Results from the ocean model when both ocean dynamics ($h_e = 50 \text{ m}$) and cloud feedbacks ($dQ_s/dT = 15 \text{ W m}^{-2} \text{ K}^{-1}$) are included. (bottom) Observed SSTs for the Pacific Ocean from Levitus and Boyer (1994).

particular the cold tail, requires a model with more complete seasonally varying ocean and atmosphere physics.

5. Discussion

Pierrehumbert (1995) suggested that the size of the warm pool (the area of the ocean where atmospheric deep convection occurs) is a key factor in the regulation of the tropical climate. He argued that this region acts as a “furnace” for the Tropics because the high humidity there traps longwave radiation. To balance this radiative heating, the atmosphere transports heat to drier regions (the subtropics), and it follows that the ratio of the area of moist to dry regions of the atmosphere determines the mean temperature of the Tropics. In his study, however, Pierrehumbert did not offer any particular physical mechanisms that would control this ratio. Herweijer et al. (2004) used the same atmospheric GCM experiments shown here (Figs. 3 and 4) to argue that, in the absence of ocean heat transports, the convecting region of the atmosphere (and the warmest water) is confined to a smaller region of the Tropics on the equator. The relative humidity in this region is very high, but low in the surrounding regions. In contrast, when ocean dynamics are included, the convection is spread over a broader meridional extent (as is the warm pool). In this case, there are large regions where the relative humidity has more intermediate values. Here water vapor can accumulate without getting close to saturation and being removed by precipitation, resulting in a moister subtropical free troposphere. The moistening of the subtropics when the ocean is allowed to move heat results in a warmer global mean temperature. In this paper, we have shown that both clouds and ocean dynamics are important in determining the distribution (both statistical and geographic) of the warmest SSTs. Inclusion of these processes results in a broad area of homogenous SSTs and, following on the arguments of Pierrehumbert (1995) and Herweijer et al. (2005), would lead to a moister and warmer atmosphere. Can these processes drive changes in the warm pool that can alter the climate?

It is difficult to envision how cloud feedbacks can generate changes in warm pool on their own. Lindzen et al. (2001) have suggested that cloud microphysics can vary with climate change. If the strength of the cloud feedback (e.g., dQ_s/dT) were to vary over time, it is possible that the distribution of warm water (and convection) would change. However, the hypothesis advanced by Lindzen et al. has been called into question on observational grounds (Chambers et al. 2002; Fu et al. 2002; Hartmann and Michelsen 2002; Lin et al. 2002;

Del Genio and Kovari 2002), and little is known about the controls on cloud microphysics. Sensitivity experiments with coupled GCMs would be useful in evaluating the ability of cloud microphysical changes to affect the structure of the warm pool.

Can changes in ocean circulation lead to variations in the size of the warm pool? We have shown here that, in the extreme case where the ocean transports no heat and all of the poleward heat transport occurs in the atmosphere, the warm pool is effectively eliminated (Fig. 3), resulting in a colder mean climate (Clement and Seager 1999; Herweijer et al. 2005). This is obviously an unrealistic extreme since under any easterly wind stress the ocean will transport some heat poleward, relieving the burden on the atmosphere of doing it all. However, it does suggest that, if the partitioning of heat transport between the ocean and atmosphere were to change, the size of the warm pool and the mean climate would be affected. Held (2001) argued that dynamical constraints at the ocean–atmosphere interface require that the transport of heat by the atmosphere and the wind-driven circulation in the ocean be approximately the same. It follows from that study that the partitioning is unlikely to vary. However, the ocean heat transport associated with the Sverdrup circulation is not as tightly constrained. Hazeleger et al. (2001, 2004) have shown that the equatorward heat transport by the tropical ocean gyres is also important and potentially disrupts the one-to-one relationship of the atmosphere and ocean heat transports. Changes in the mean depth of the thermocline can alter the Sverdrup component of the oceanic heat transport, and the structure of the warm pool as demonstrated in Fig. 9. Ideas are only now being advanced for what controls the mean depth of the equatorial thermocline, which show that it is strongly influenced by the global distribution of surface buoyancy fluxes (Boccaletti et al. 2004). Philander and Fedorov (2003) argue that the mean equatorial thermocline has been significantly deeper at times in the past. If so, this has potentially significant implications for the ability of the size and structure of the warm pool to vary and affect the mean climate. Further studies, in particular with coupled GCMs, are required to understand the relationship between the partitioning of ocean–atmosphere heat transport and the size of the warm pool more completely.

6. Conclusions

The model results presented here provide a framework for understanding the contributions of different atmospheric and oceanic processes to the establishment of tropical warm pools. They can be summarized as follows.

- The response of local processes to the distribution of incoming solar radiation results in a highly skewed tropical SST distribution. Unlike the observed distribution, however, under purely local balance the most common SST would be the highest one. This implies that nonlocal processes must cool the warmest SSTs.
- With the inclusion of nonlocal atmospheric processes (i.e., circulation), as demonstrated with a GCM, the atmosphere responds to the distribution of solar radiation by transporting heat poleward via the Hadley cell. The heat transport itself will tend to preferentially cool the warmest SST, which would homogenize the SST. However, the circulation also results in a moist deep convecting region with low wind speeds and dry subtropics with high wind speeds. These effects tend to remove homogeneity from the SST, and the net effect of these atmospheric processes is a SST distribution that has no peak at all.
- Under the easterly wind stress of the Hadley cell, ocean dynamics homogenize the tropical SST. Surface Ekman drift moves water from regions of maximum solar heating (in the absence of clouds) on the equator and converges heat in the off-equatorial regions. As a result of the east–west tilt of the thermocline, the water that replaces this poleward drift is relatively cold in the east, creating a cold tongue, and warm in the west, homogenizing SST and creating a warm pool. For a reasonable choice of mean equatorial thermocline depth, these dynamical processes in the ocean can explain the main features of the observed SST distribution, though with a somewhat weaker peak.
- High clouds can also homogenize tropical SST by reducing the absorbed solar radiation over the warmest SSTs. By parameterizing this feedback in a simplified way, we demonstrate that such a cloud feedback can offset the effect of the off-equatorial cooling by atmospheric processes and homogenize the tropical SST, resulting in a distribution similar to the observed, though also with a weaker peak. There are, however, large uncertainties about how this feedback operates and about its strength.
- For reasonable parameter values, the simple ocean model with a high cloud feedback produces an SST distribution that is in good agreement with the observed for the Pacific. Thus, it appears that both ocean dynamics and cloud feedbacks are fundamental to the existence of a warm pool.

The results presented here suggest that the warm pool can be modeled with a relatively small set of ocean and atmosphere processes. However, we have not included the potentially important effects of the seasonal cycle

and complete dynamical coupling between the ocean and atmosphere. Future work will focus on the development of a simplified coupled model to test our findings in the context of the more complete, seasonally varying, coupled system.

Acknowledgments. The authors thank Adam Sobel and two anonymous reviewers for extremely insightful comments on an earlier version of the paper. AC and RS were supported by NOAA-ARCHES UCSIOCU-02165401SCF. AC received additional support from a National Science Foundation Paleoclimate Program Grant (ATM-0134742), and a NASA Grant (NNG04GM67G). RS received support from NSF ATM-9986072. RM was supported by a NASA Salinity Grant and a NOAA Monsoon Grant.

APPENDIX

Idealized Ocean Model

The model consists of a single layer of variable depth $h = h_1 - h_2$ and constant density ρ_1 . This is assumed to overlie a motionless layer of constant density ρ_2 . The derivation of the thermocline depth follows that of Veronis (1973). The pressure gradients can be rewritten in terms of the gradient in layer depths:

$$\frac{1}{\rho_1} \nabla p_1 = g \nabla h_1 \quad (\text{A1})$$

$$\frac{1}{\rho_2} \nabla p_2 = g \left(\frac{\Delta \rho}{\rho_2} \nabla h_2 + \frac{\rho_1}{\rho_2} \nabla h_1 \right), \quad (\text{A2})$$

where $\Delta \rho = \rho_2 - \rho_1$. The meridional wind stress, τ^e , is taken to be zero everywhere, and the zonal wind stress $\tau^\lambda = \tau$ at the surface and goes to zero at h_2 , the base of the upper layer. Since the lower layer is quiescent, $\nabla p_2 = 0$ and

$$\nabla h_1 = \frac{\Delta \rho}{\rho_2} \nabla h. \quad (\text{A3})$$

The zonal pressure gradient can then be written in the reduced gravity formulation as

$$\frac{1}{\rho_1} \frac{\partial p_1}{\partial \lambda} = g' \frac{\partial h}{\partial \lambda}, \quad (\text{A4})$$

where $g' = g \Delta \rho / \rho_2$. The momentum and continuity equations are now written as

$$-fv = -\frac{1}{a \cos \varphi} g' \frac{\partial h}{\partial \lambda} + \frac{\partial \tau}{\partial z} \quad (\text{A5})$$

$$fu = -\frac{1}{a} g' \frac{\partial h}{\partial \varphi} \quad (\text{A6})$$

$$\frac{\partial u}{\partial \lambda} + \frac{\partial}{\partial \varphi}(v \cos \varphi) + a \cos \varphi \frac{\partial w}{\partial z} = 0. \quad (\text{A7})$$

Vertically integrating, these become

$$-fV = -\frac{g'}{a \cos \varphi} \frac{\partial}{\partial \lambda} \left(\frac{h^2}{2} \right) + \tau \quad (\text{A8})$$

$$fU = -\frac{g'}{a} \frac{\partial}{\partial \varphi} \left(\frac{h^2}{2} \right) \quad (\text{A9})$$

$$\frac{\partial U}{\partial \lambda} + \frac{\partial}{\partial \varphi}(V \cos \varphi) = 0, \quad (\text{A10})$$

where U and V are the total transports. Taking the curl of the velocities, we recover the Sverdrup relation:

$$V = \frac{1}{a\beta \cos \varphi} \frac{\partial}{\partial \varphi} (\tau \cos \varphi). \quad (\text{A11})$$

Substituting into the above equation for V , we can write an equation for h :

$$\frac{\partial}{\partial \lambda} \left(\frac{h^2}{2} \right) = \frac{a}{g'} \left[\frac{\sin \varphi}{\cos \varphi} \frac{\partial}{\partial \varphi} (\tau \cos \varphi) + \tau \cos \varphi \right]. \quad (\text{A12})$$

Assuming $h = h_e$ along the eastern boundary and zonally integrating, we get

$$h^2(\lambda, \varphi) = h_e^2(\lambda_e, \varphi) - \frac{2a}{g'} \times \left[\frac{\sin \varphi}{\cos \varphi} \frac{\partial}{\partial \varphi} (\tau(\varphi) \cos \varphi) + \tau(\varphi) \cos \varphi \right] (\lambda_e - \lambda) \quad (\text{A13})$$

and along the equator, since $\varphi = 0$,

$$h^2(\lambda) = h_e^2 - \frac{2a}{g'} \tau_{\text{eq}} (\lambda_e - \lambda). \quad (\text{A14})$$

Since $\tau_{\text{eq}} < 0$, $h^2 > h_e^2$, the thermocline deepens linearly to the west.

To calculate the mixed layer temperature, first we need to know the currents in the mixed layer. These are derived for Ekman balance with linear damping r_s as in Zebiak and Cane (1987) and Seager et al. (1988), assuming a fixed mixed layer depth, H , of 50 m and that $\tau^\varphi = 0$, so

$$v_s = \frac{-f\tau}{(r_s^2 + f^2)\rho H}, \quad u_s = \frac{-r_s v_s}{f}. \quad (\text{A15})$$

The depth averaged flow is

$$\mathbf{u} = \frac{1}{h} (h_1 \mathbf{u}_1 + h_2 \mathbf{u}_2), \quad (\text{A16})$$

and the Ekman flow is

$$\mathbf{u}_s = \mathbf{u}_1 - \mathbf{u}_2 \quad (\text{A17})$$

so that we can compute total currents that can be used in the mixed layer temperature equation:

$$\mathbf{u}_1 = \mathbf{u}_s \frac{h_2}{h} + \mathbf{u}. \quad (\text{A18})$$

By continuity, we can calculate the upwelling into the surface layer using \mathbf{u}_1 :

$$w_s = \frac{H}{a \cos \varphi} \left(\frac{\partial u_1}{\partial \varphi} + \frac{\partial}{\partial \varphi} (v_1 \cos \varphi) \right). \quad (\text{A19})$$

A mixed layer temperature is then computed using these surface layer currents, as in the earlier studies of Zebiak and Cane (1987) and Seager et al. (1988):

$$\frac{\partial T_s}{\partial t} + \frac{u_1}{a \cos \varphi} \frac{\partial T_s}{\partial \lambda} + \frac{v_1}{a} \frac{\partial T_s}{\partial \varphi} + \gamma M(w_s) \frac{(T_s - T_d)}{H} = \frac{Q}{\rho c_p H} + \nu \nabla^2 T_s. \quad (\text{A20})$$

It is assumed, as in earlier studies, that the temperature of the upwelling water, T_d , is a function of the depth of the thermocline; only here we assume for simplicity that it is a linear function: M is a function that is unity when there is upwelling ($w_s > 0$) and zero when there is downwelling. Values for parameters are $\gamma = 0.75$ and $\nu = 1 \times 10^4 \text{ m s}^{-1}$. The surface heat flux is calculated as

$$\begin{aligned} Q &= Q_r - Q_{\text{LH}} - \alpha(T_s - T^*) \\ &= Q_r - \rho_a c_e L |\underline{u}| (1 - \delta) q_s - \alpha(T_s - T^*), \end{aligned} \quad (\text{A21})$$

where Q_r is the net surface solar radiation and δ is the relative humidity, which decreases from a value of 80% at the equator as $\cos \varphi^{-2}$, similar to the observed. The wind speed used to calculate the surface latent heat flux, $|\underline{u}|$, is the total wind speed (unlike the wind stress term that only uses the zonal wind). The term $\alpha(T_s - T^*)$ represents sensible heat loss and longwave radiation. Parameter values are $\alpha = 1.5 \text{ W m}^{-2} \text{ K}^{-1}$ and $T^* = 273.15 \text{ K}$. This is a similar formulation to Seager et al. (1988), but here the net surface solar radiation is specified to be a function of latitude. The values for all other parameters are the same as those used in Seager et al. (1988).

REFERENCES

- Betts, A. K., and W. Ridgway, 1989: Climatic equilibrium of the atmospheric convective boundary layer over a tropical ocean. *J. Atmos. Sci.*, **46**, 2621–2641.
- Bjerknes, J., 1966: A possible response of the atmospheric Hadley

- circulation to equatorial anomalies of ocean temperature. *Tellus*, **18**, 820–829.
- Boccaletti, G., R. C. Pacanowski, S. G. H. Philander, and A. V. Federov, 2004: The thermal structure of the upper ocean. *J. Phys. Oceanogr.*, **34**, 888–902.
- Cane, M. A., and E. S. Sarachik, 1976: Forced baroclinic ocean motions I: The linear equatorial unbounded case. *J. Mar. Res.*, **34**, 629–664.
- Chambers, L., B. Lin, B. Wielicki, Y. X. Hu, and K. M. Xu, 2002: Reply. *J. Climate*, **15**, 2716–2717.
- Clement, A. C., and R. Seager, 1999: Climate and the tropical oceans. *J. Climate*, **12**, 3384–3401.
- , —, M. A. Cane, and S. E. Zebiak, 1996: An ocean dynamical thermostat. *J. Climate*, **9**, 2190–2196.
- da Silva, A., A. C. Young, and S. Levitus, 1994: *Algorithms and Procedures*. Vol. 1, *Atlas of Surface Marine Data 1994*, NOAA Atlas NESDIS 6, 83 pp.
- Del Genio, A. D., and W. Kovari, 2002: Climatic properties of tropical precipitating convection under varying environmental conditions. *J. Climate*, **15**, 2597–2615.
- Dijkstra, H. A., and J. D. Neelin, 1995: Ocean–atmosphere interaction and the tropical climatology. Part II: Why the Pacific cold tongue is in the east. *J. Climate*, **8**, 1343–1359.
- Fu, Q., M. Baker, and D. L. Hartmann, 2002: Tropical cirrus and water vapor: An effective Earth infrared iris feedback? *Atmos. Chem. Phys.*, **2**, 31–37.
- Fu, R., A. D. DelGenio, W. B. Rossow, and W. T. Liu, 1992: Cirrus cloud thermostat for tropical sea surface temperatures tested using satellite data. *Nature*, **358**, 394–397.
- Hartmann, D. L., and M. L. Michelsen, 1993: Large-scale effects on the regulation of tropical sea surface temperature. *J. Climate*, **6**, 2049–2062.
- , and —, 2002: No evidence for iris. *Bull. Amer. Meteor. Soc.*, **83**, 249–254.
- , M. E. Ockert-Bell, and M. Michelsen, 1992: The effect of cloud type on earth's energy balance: Global analysis. *J. Climate*, **5**, 1281–1304.
- , L. A. Moy, and Q. Fu, 2001: Tropical convection and the energy balance at the top of the atmosphere. *J. Climate*, **14**, 4495–4511.
- Hazeleger, W., M. Visbeck, M. A. Cane, A. Karspeck, and N. Naik, 2001: Decadal upper ocean temperature variability in the tropical Pacific. *J. Geophys. Res.*, **106** (C5), 8971–8988.
- , R. Seager, M. Cane, and N. Naik, 2004: How can tropical Pacific ocean heat transport vary? *J. Phys. Oceanogr.*, **34**, 320–333.
- Held, I. M., 2001: The partitioning of the poleward energy transport between the tropical ocean and atmosphere. *J. Atmos. Sci.*, **58**, 943–948.
- Herweijer, C., R. Seager, and M. Winton, 2005: Why ocean heat transport warms the global mean climate. *Tellus*, **57A**, 662–675.
- Kiehl, J. T., J. J. Hack, G. B. Bonan, B. P. Boville, D. L. Williamson, and P. J. Rasch, 1998: The National Center for Atmospheric Research Community Climate Model: CCM3. *J. Climate*, **11**, 1131–1149.
- Klein, S. A., and D. L. Hartmann, 1993: The seasonal cycle of low stratiform clouds. *J. Climate*, **6**, 1587–1606.
- Larson, K., and D. L. Hartmann, 2003: Interactions among cloud, water vapor, radiation, and large-scale circulation in the tropical climate. Part II: Sensitivity to spatial gradients of sea surface temperature. *J. Climate*, **16**, 1441–1455.
- , —, and S. A. Klein, 1999: On the role of clouds, water vapor, circulation, and boundary layer structure on the sensitivity of the tropical climate. *J. Climate*, **12**, 2359–2374.
- Lau, K.-M., C.-H. Sui, M. D. Chou, and W.-K. Tao, 1994: An inquiry into the cirrus-cloud thermostat effect for tropical sea surface temperature. *Geophys. Res. Lett.*, **21**, 1157–1160.
- Levitus, S., and T. P. Boyer, 1994: *Temperature*. Vol. 4, *World Ocean Atlas 1994*, NOAA Atlas NESDIS 4, 117 pp.
- Lin, B., B. A. Wielicki, L. H. Chambers, Y. X. Hu, and K. M. Xu, 2002: The iris hypothesis: A negative or positive cloud feedback? *J. Climate*, **15**, 3–7.
- Lindzen, R. S., M. D. Chou, and A. Y. Hou, 2001: Does the earth have an adaptive infrared iris? *Bull. Amer. Meteor. Soc.*, **82**, 417–432.
- Ma, C.-C., C. R. Mechoso, A. W. Robertson, and A. Arakawa, 1996: Peruvian stratus clouds and the tropical Pacific circulation: A coupled ocean–atmosphere GCM study. *J. Climate*, **9**, 1635–1645.
- Miller, R. L., 1997: Tropical thermostats and low cloud cover. *J. Climate*, **10**, 409–440.
- Peixoto, J. P., and A. H. Oort, 1992: *Physics of Climate*. American Institute of Physics, 520 pp.
- Philander, S. G., and A. V. Fedorov, 2003: The role of tropics in changing the response to Milankovich forcing some three million years ago. *Paleoceanography*, **12**, 1045, doi:10.1029/2002PA000837.
- Pierrehumbert, R. T., 1995: Thermostats, radiator fins, and the runaway greenhouse. *J. Atmos. Sci.*, **52**, 1784–1806.
- Ramanathan, V., and W. Collins, 1991: Thermodynamic regulation of ocean warming by cirrus clouds deduced from observations of the 1987 El Niño. *Nature*, **351**, 27–32.
- Salathe, E. P., and D. L. Hartmann, 1997: A trajectory analysis of tropical upper-tropospheric moisture and convection. *J. Climate*, **10**, 2533–2547.
- , and —, 2000: Subsidence and upper-tropospheric drying along trajectories in a general circulation model. *J. Climate*, **13**, 257–263.
- Seager, R., S. E. Zebiak, and M. A. Cane, 1988: A model of the tropical Pacific sea surface temperature climatology. *J. Geophys. Res.*, **93**, 1265–1280.
- , A. C. Clement, and M. A. Cane, 2000: Glacial cooling in the Tropics: Exploring the roles of tropospheric water vapor, surface wind speed, and boundary layer processes. *J. Atmos. Sci.*, **57**, 2144–2157.
- , R. Murtugudde, A. C. Clement, and C. Herweijer, 2003a: Why is there an evaporation minimum at the equator? *J. Climate*, **16**, 3792–3801.
- , —, N. Naik, A. Clement, N. Gordon, and J. A. Miller-Velez, 2003b: Air–sea interaction and the seasonal cycle of the subtropical anticyclones. *J. Climate*, **16**, 1948–1966.
- Sobel, A. H., 2003: On the coexistence of an evaporation minimum and precipitation maximum in the warm pool. *J. Climate*, **16**, 1003–1009.
- , I. M. Held, and C. S. Bretherton, 2002: The ENSO signal in tropical tropospheric temperature. *J. Climate*, **15**, 2702–2706.
- Soden, B. J., 1997: Variations in the tropical greenhouse effect during El Niño. *J. Climate*, **10**, 1050–1055.
- Sun, D.-Z., and Z. Liu, 1996: Dynamic ocean–atmosphere coupling: A thermostat for the tropics. *Science*, **272**, 1148–1150.
- Trenberth, K. E., and J. M. Caron, 2001: Estimates of meridional

- atmosphere and ocean heat transports. *J. Climate*, **14**, 3433–3443.
- Veronis, G., 1973: Model of world ocean circulation: 1. Wind-driven, two layer. *J. Mar. Res.*, **31**, 228–288.
- Waliser, D. E., and N. E. Graham, 1993: Convective cloud systems and warm-pool sea-surface temperatures—Coupled interactions and self-regulation. *J. Geophys. Res.*, **98D**, 12 881–12 893.
- Wallace, J. M., 1992: Effect of deep convection on the regulation of tropical sea surface temperature. *Nature*, **357**, 230–231.
- Winton, M., 2003: On the climatic impact of ocean circulation. *J. Climate*, **16**, 2875–2889.
- Wyrtki, K., 1975: El Niño—The dynamic response of the equatorial Pacific Ocean to atmospheric forcing. *J. Phys. Oceanogr.*, **5**, 572–584.
- Zebiak, S. E., and M. A. Cane, 1987: A model El Niño–Southern Oscillation. *Mon. Wea. Rev.*, **115**, 2262–2278.
- Zhang, G. J., V. Ramanathan, and M. J. McPhaden, 1995: Convection–evaporation feedback in the equatorial Pacific. *J. Climate*, **8**, 3040–3051.